A Strategy for the Maximum Fluorescence Enhancement Based on Tetrahedral Amorphous Carbon-Coated Metal Substrates

Fanxin Liu,* Chaojun Tang, Jian Pan, Zhishen Cao, and Zhenlin Wang*

National Laboratory of Solid State Microstructures and Department of Physics, Nanjing University, Nanjing 210093, P. R. China

Received: February 26, 2010; Revised Manuscript Received: April 22, 2010

Recently metal-enhanced fluorescence (MEF) has been reported. However, the bare metal would always quench the emission if the separation between the fluorophore and metal is very close. In order to get maximum fluorescence enhancement, the key point is to allow the maximum local electric field of plasmonic substrate at the interface to be used, and at the same time the quenching should be efficiently reduced. We demonstrate for the first time that by coating with an ultrathin dielectric layer of tetrahedral amorphous carbon (ta-C), an optically transparent material in the visible, the metal nanostructures can be used to realize the maximum enhancement in MEF. This result can be attributed to the well control of two competitive mechanisms of the local field enhancement and quenching. It is found that a 10 Å ta-C layer can modify plasmon resonance of the metal to produce a higher local electric field than uncoated metal and can also reduce the quenching. The coated metal substrate has higher mechanical stability, chemical inertness, and technological compliance and may be useful, for example, to enhance TiO_2 photocatalysis and solar-cell efficiency and to design the surface plasmon laser with fluorophores as gains by the surface plasmons.

Introduction

Noble metal nanoparticles (MNPs) exhibit unique, remarkably vivid optical properties due to excitation of their surface plasmon (SP) mode by incident light.[1] Plasmon excitation results in significantly enhanced local electric fields at the nanoparticle surfaces, which gives rise to fundamentally interesting phenomena and technologically important applications[2−9] such as MEF.[10−17] MEF is the modification of the fluorescence intensities and lifetimes for fluorophores placed near a metal surface,[18−20] which has attracted special attention from the viewpoints of academic as well as industrial interests. There are two competitive mechanisms at work which are both dependent on the separation distance between the fluorophores and metal surfaces.[19,20] One is the quenching due to electron transfer[21] or nonradiative energy transfer (as in Föster's theory)[22−25] from the fluorophores to the metal. In the case of fluorophores located at very short distances or direct contact from a metal surface, distinct enhancement of the nonradiative deacy owing to ohmic losses in the metal due to electron transfer from the fluorophores to metal trapping results in an overall quenching of the luminescence.[22] As the separation is increased to a few nanometers, the quenching will be rapidly reduced and then return to its unperturbed value.[20,22] Another is the electric field enhancement mechanism through the Purcell effect[26] which takes place at the stages of optical excitation and the fluorescence emission. At the optical excitation stage, the incident light can get coupled first into the tightly confined SP mode of MNPs enhancing the optical energy density near the fluorophores field, which results in significant increases in their absorption rate.[27] The same SP mode can also get coupled with the emission band of fluorophores inducing the enhanced local electric field, which greatly enhances their emission rate.[28] Both the absorption and emission processes are dependent on the intensity of local electric field surrounding the MNPs under illumination, which is the maximum at the interface between MNPs and fluorophores and decays exponentially in the directions perpendicular to the interface.[1] As a result, the separation distance is chosed properly to get the optimum MEF because the local field enhancement due to SP still occurs at longer distances from the metal surface.[21,29] Now, though the local field is only partly used, considerable efforts have been made to control this distance to acquire the fluorescent enhancement. For example, a metal-core/silica-shell colloidal nanoparticle was developed to be used as bright fluorescent markers with enhanced photostability in fields such as biodetection and fluorescent microscopy.[30] Another, in immobilized substrates of noble-metal nanoparticles, fluorophores mixed with PMMA were spin-coated with a thickness of around 30 nm, which induces a MEF enhancement.[31]

To obtain the maximum MEF enhancement, how to allow the maximum local field at the interface to be used is the key point. Here, we report a strategy that by coating with an ultrathin dielectric layer of ta-C, a biocompatible and optically transparent material in the visible, the metal nanostructured substrate can be used to realize the maximum enhancement of photoluminescence (PL) of quantum dots (QDs). It is found that the ultrathin ta-C layer can modify the SP mode of metal nanoparticle to produce a higher local electric field than the bare metal substrate[32−34] and also can efficiently prevent electron transfer from QDs to metal surface so that the quenching is reduced, as shown in Figure 1. This coated substrate also has higher mechanical stability, chemical inertness, and technological compliance and may be useful, for example, to enhance TiO_2 photocatalysis[35] and solar-cell efficiency[36,37] by the surface plasmons. In addition, this strategy due to providing the maximum fluorescence enhancement can be used to design the surface plasmon laser with fluorophores as gains,[38,39] even possible at room temperature.

Diamond-like carbon (DLC) film is an amorphous carbon material which contains a mixture of sp^3-bonded (as in diamond)

* Corresponding authors. E-mail: lfx63@163.com (F.L.), zlwang@nju.edu.cn (Z.W.).

10.1021/jp101767z
Published on Web 05/11/2010

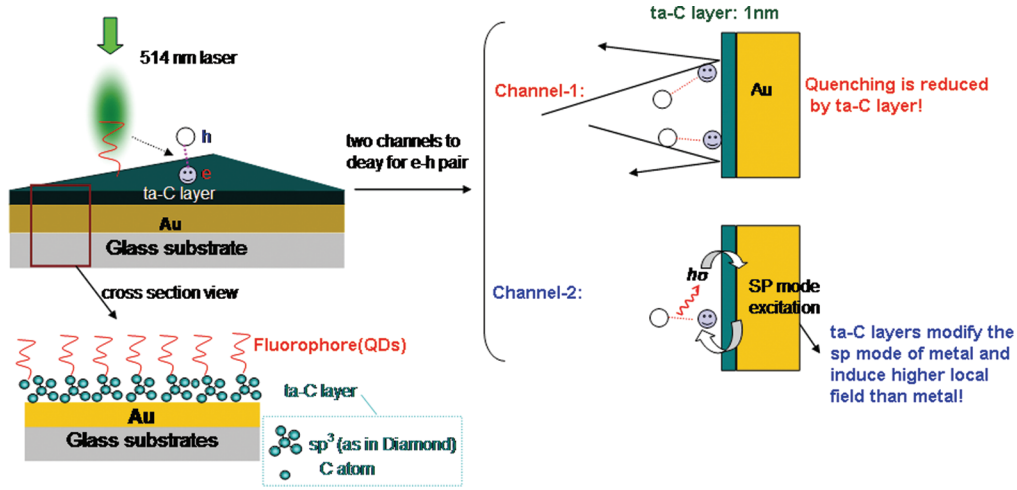

Figure 1. Schematic illustration of fluoropheres adsorbed on the ta-C layer coated metal substrate and its PL process: the electron−hole pairs from the fluorophores excited by incident laser have two channels to decay. Channel 1 is quenching, and channel 2 is local field enhancement.

and sp^2-bonded (as in graphite) carbon atoms.[40] Numerous types of DLC films such as hydrogenated amorphous carbon (a-C:H), ta-C, etc., can be deposited using a variety of plasma deposition technologies.[41] But only ta-C film with sp^3 bonding up to 90% and a thickness up to 1−2 nm can preserve its extraordinary mechanical properties, thus serving as a protective coating layer.[40−42] The ta-C film as an ultrathin film has many desirable properties, such as pinhole free, chemical inertness, thermal stability, biocompatibility, high electrical resistance, and optical transparency in the visible and infrared, etc.[40] Compared with polycrystalline diamond,[41] a ta-C film also has distinct advantage in that it can be deposited at room temperature. Another advantage is that ta-C film is atomically smooth and generally takes on the roughness of the substrate on which it is deposited, which is highly desirable for many optical and biomedical applications.[43,44]

Experimental Section

Gold Nanoparticle Substrates Fabrication. In our experiment, the Au-based substrates were fabricated using nanosphere lithography (NSL) as described previously.[45] Monodisperse polystyrene nanospheres (PSs) (508 nm and 1.6 μm diameter, Duke Scientific) were drop-coated onto a cleaned and base-treated glass substrate and were allowed to dry, forming a hexagonal close-packed monolayer which served as a deposition mask. Au (99.999% purity) was then sputtered on the top of the nanospheres in a vacuum chamber. Subsequent removal of the nanosphere mask via tape stripping left a highly ordered array of relatively uniform triangular gold nanoparticles.

ta-C Films Deposition. The Au prepared nanoparticles substrates were further coated with an ultrathin ta-C film using a multifilm deposition system (Shimadzu, MR3, in SAE Magnetics (H.K) Ltd.)) with the combination of a FCVA (filtered cathodic vacuum arc) gun (Nanofilm Technology International, Singapore).[41,42] The deposition rate monitored by an ellipsometer was ∼0.5 Å/s, and the film thickness was varied from 5 to 40 Å. Prior to deposition, all the substrates were cleaned by RF-plasma sputtering using Ar ion plasma. The refractive index of ta-C film was measured to be ∼2.3 in the spectrum range from 400 to 1000 nm. In addition, the refractive index of ta-C films almost had no change from 5 to 40 Å. A water contacted angle (WCA) of ∼68° of the ta-C film was measured, which shows that the prepared ta-C films are hydrophilic. After films deposition, the roughness has a ∼0.5 Å increase due to ion beam sputtering for cleaning before coating (data not shown here).

Characterizations and QDs PL Testing. The morphology of Au nanoparticles was explored with a Digital Instrument Nanoscope atomic force microscope (AFM) in tapping mode. In the experiment, water-soluble CdSe/ZnS QDs (10^{-9} M) with an emission peak centered at 595 nm was used. For allowing the QDs adsorption the prepared substrates were maintained for 20 h into QDs solution and then taken out and dried with nitrogen gas to creat a disperse film of QDs. The PL spectra of QDs were acquired by using a Renishaw Invia Raman microscope system with an excitation wavelength at $\lambda = 514$ nm with 0.02 mW laser output power, 10 s collection time, and a 50× magnification objective.

Results and Discussion

In our experiment, the Au nanoparticles substrates were fabricated using NSL as described previously with the template spheres of diameters of 508 nm and 1.6 μm.[45] Although enhanced emission of Ag based substrate was observed, Au coating is more desirable because it is commonly used as the electrode material for electronic devices. Then these substrates were coated with an ultrathin ta-C film. Figure 2 shows the morphology of the Au nanoparticles substrates coated with a 10 Å ta-C film. Measurements show that the width of the nanoparticles along the perpendicular bisector is ∼130 nm (508 nm PSs mask) and ∼426 nm (1.6 μm PSs mask), and the height is ∼40 nm. In addition, the prepared Au nanoparticle arrays show no observable deformation after coating due to low-temperature plasma deposition. Such nanoparticles exhibit larger local field enhancements than spherical particles and their sharp edges lead to more effective coupling of the SP mode to far-field radiation, which is useful to enhance emission of fluorophores.

Figure 3 presents the enhanced PL spectra of QDs on these ta-C layer coated Au nanoparticles substrates, compared to a reference with QDs on the same ta-C layer coated glass slide. It is noted here that only the samples prepared with 1.6 μm PSs mask are selected for studying the fluorescence enhancement dependence on the ta-C layer thickness because we used an extreme thin layer of ta-C, which was changed from 5 to 40 Å. Although we can grow PS colloidal crystal templates from 508 nm or 1.6 μm diameter PS microspheres, the 1.6 μm diameter PS templates have fewer defects, and the measured

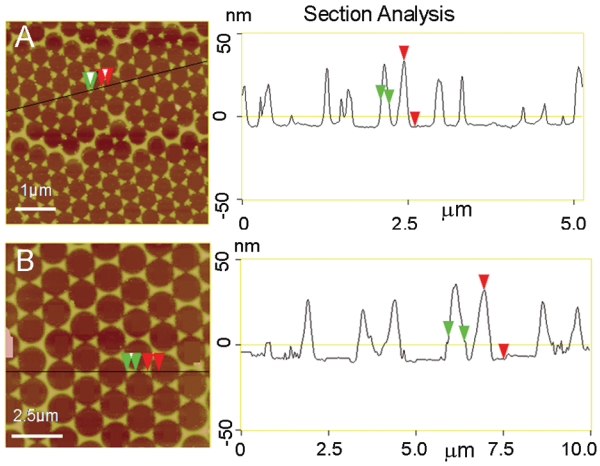

Figure 2. AFM image of Au nanoparticles substrate coated with ta-C films thickness of 10 Å, prepared with 508 nm PSs mask (A) and 1.6 μm PSs mask (B).

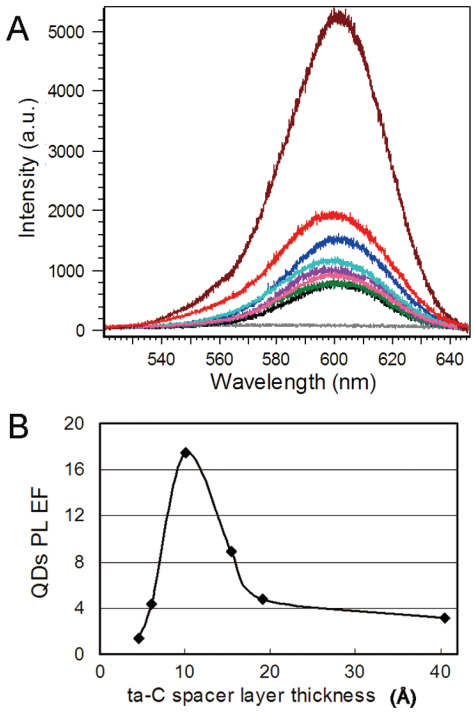

Figure 3. (A) QDs PL spectra on the following substrates: the Au film (gray line); the ta-C coated glass as a reference (black line); the 10 Å ta-C coated Au nanoprisms prepared with 508 nm mask (purple line); and the Au nanoprisms prepared with 1.6 μm PSs mask coated with the ta-C with the thickness of 10.1 (red line), 15.5 (blue line), 19.1 (aqua green), 6.1 (sepia line), 40.5 (pink line), and 4.6 Å (green line). (B) QDs PL enhancement factor (EF) as a function of ta-C spacer layer thickness on the Au nanoprisms substrates prepared with 1.6 μm PSs mask.

results show good repeatability and thus are more accurate. The 508 nm diameter PS templates have more defects as compared with the 1.6 μm diameter PS templates. Random interlinked nanoprisms or long metal strips will be formed when the 508 nm diameter PS microspheres are used (as shown in Figure 2A). In addition, only one sample with 508 nm PSs mask coated with a 10 Å ta-C layer checked by AFM is used to study the size-dependent MEF enhancement. From the Figure 3A, the QDs emission is completely quenched when the QDs is directly placed on the Au films. However, when the substrates are coated with ta-C layer, the PL spectra of QDs show the enhancement. By careful observation, the emission peak position almost did not shift despite the fluorescence intensity increased. Figure 3A also shows that for the substrate coated with the 10 Å ta-C layer the intensity of the PL spcectra on the substrate with 508 nm PSs mask is ~4 times higher than that on the substrate with 1.6 μm PSs mask. To further compare the MEF effect dependent on the thickness of ta-C layer, we calculate the absolute enhancement factors (EF) based on the following formula: EF $= I_{\text{coated-subst}}/I_{\text{coated-glass}}$, where $I_{\text{coated-subst}}$ and $I_{\text{coated-glass}}$ are the conventional PL intensities on the coated Au nanoparticles substrates and glass substrate, respectively. During the calculation, the absoluted intensity that does not include the blank area is deduced by considering the focus spot size and the Au nanoparticle size. The EF as a function of the thickness of ta-C film on the substrates prepared with 1.6 μm dimeter PSs mask is shown in Figure 3B. The data show that the EF on the coated Au-based substrate reaches a maximum at the 10 Å ta-C layer (a 17-fold increase).

To understand the origin of PL enhancement of QDs dependence on particle sizes, we measured the transmittance spectra for Au nanoparticles substrates coated with the ta-C films under normal incidence of an unpolarized light, shown in Figure 4. For these uniform Au nanoparticles with 508 nm dimeter PSs mask coated with the 10 Å ta-C layer, the transmittance in Figure 4A shows two broad bands centered at ca. 640 and 430 nm, which are due to the dipole and quadrupole resonance of the Au nanoparticles.[46] Similarly, for Au nanopatricles with 1.6 μm dimeter PSs mask, Figure 4B shows that the dipole and quadrupole peaks are located at 2240 and 1390 nm,[45] respectively. A red shift in the plasmon dipole resonance peak from 2240 (without ta-C layer) to 2260 nm (with a 10 Å ta-C layer) is also observed[47] in Figure 4B, which indicates that changes to the local dielectric environment beyond a certain short distance from the surface do not apparently affect the SP of Au nanoparticles. This localized SP resonance leads a locally enhanced electral field which is responsible for the enhanced PL of QDs. Compared with the coated Au nanoparticles prepared with 1.6 μm PSs mask, it is found that the dipole band of the 10 Å ta-C layer coated Au nanoparticles with 508 nm PSs mask is remarkable overlap with the PL band of QDs, which strongly supports the high efficiency of the MEF observed in our experiment.[28,48] This good agreement proves a dependence of the enhancement efficiency on the degree of spectral overlap between the plasmon resonance of the nanoparticles and the PL band of QDs. This is an indication that the enhancement is due to the near-field coupling between the fluorophore dipole and SP electronic oscillations at the emission frequency.[18−20] Since the excitation wavelength (514 nm) is well outside the main plasmon excitation band, we expect a negligible contribution from the absorption enhancement in our experiment. In addition, although time-resolved measurements would be useful to disentangle the contributions of different enhancement pathways, in our case the substrate-dependent enhancement factors and spectral positions of localized SP resonances suggest the involvement of a plasmon-coupled emission mechanism. This electromagnetic coupling will decrease their radiative lifetime, thereby increasing their photostability.[24]

The above results also clearly show the dependence of the EF of QDs PL on the different ta-C layer thicknesses: the EF on the coated Au-based substrate was found to reach the maximum at the 10 Å ta-C layer. This result can be attributed to the two competitive mechanisms of the quenching (nonradiative decay) and local electromagnetic field induced PL enhancement. At such close separation, the nonradiative decay process prevails due to electron transfer via quantum tunnel

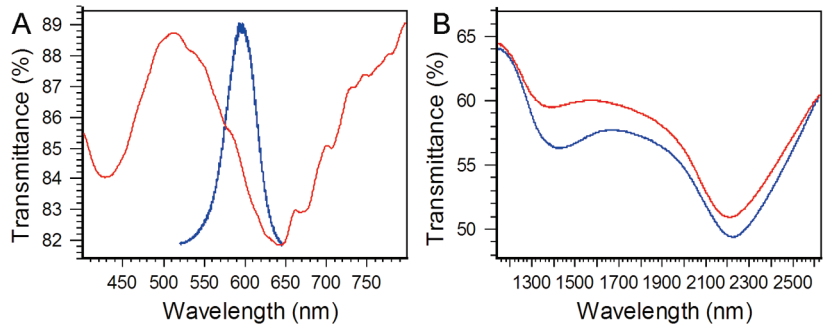

Figure 4. (A) Transmittance spectra of Au nanoparticle arrays (with 508 nm sphere mask) coated with ta-C film thickness of 10 Å (red line) and QDs PL specrum (blue line). (B) Transmittance spectra of Au nanoparticle arrays (with 1.6 μm sphere mask) (red line) and coated with ta-C film thickness of 10 Å (blue line).

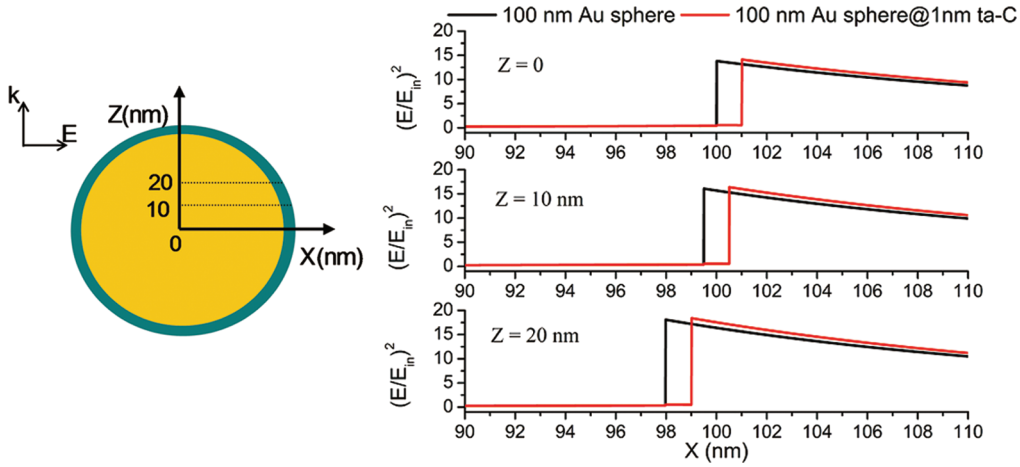

Figure 5. Distance-dependent local electromagnetic field $(E/E_{in})^2$ calculated for a Au sphere with coated ta-C film thickness of 1 nm (red line) and uncoated Au sphere (black line) ($Z = 0$, $Z = 10$ nm, and $Z = 20$ nm represent the distance from the center and bias of center 10 and 20 nm of Au sphere).

effect from the QDs to the metal.[20,21] As the separation is increased, the nonradiative decay rate will rapidly decrease and then return to its unperturbed value,[21] as shown in Figure 1S (red line) (see Supporting Information). On the other hand, the local electral field intensity of SP mode on the substrate is responsible for the enhancement of QDs's PL. This local electromagnetic field surrounding the Au nanoparticle under illumination is an evanescent wave that exponentially decays with the distance away from the metal surface which corresponds to the decay of QDs's PL with the increasing of ta-C thickness, as shown in Figure 1S (blue line).[20] As such, these two mechanisms compete with each other and thus render a distribution of total PL enhancement of QDs as a function of ta-C spacer layer thickness (Figure 1S, black dotted line), which is consistent with our experimental result. Furthermore, through the evaluation of the coverage of ta-C films on the Ag substrate, we find that a 10 Å ta-C layer is dense enough (see Supporting Information), which indicates that a 10 Å ta-C coating layer can efficiently reduce the electron transfer to metal. Considering the decaying characteristics of local electric field with the ta-C thickness, the EF on the coated Au-based substrate could reach a maximum at the 10 Å ta-C layer coated substrate.

The data show that the EF on the Au nanopartiles substrate coated with a 10 Å ta-C layer is the maximum, and a 64-fold increase is attained when the SP mode of the substrate is efficiently coupled with the QDs PL band. In previous study, the obtained maximum enhancement dependence on the separation distance is based on thicker spacer layer (such as, over 5 nm for SiO_2 layer).[30] But this thick spacer layer also makes the local field intensity outside the coated metal surface become lower than that outside uncoated metal surface.[33] Here, we will explore how a 10 Å ta-C layer modifies the plasmon resonance of the metal substrate. To do this, we have calculated the distance-dependent local electral field for an individual Au nanosphere coated with a 10 Å ta-C films and an uncoated Au nanosphere that may be considered as a reference for triangular nanoparticle. Though the shape of nanosphere is different from triangular, the effect of a dielectric layer modification to the local SP field of a metal nanoparticle surface is very similar. The field enhancements of the coated and uncoated nanospheres were calculated by the Mie theory. In this model, the Au nanosphere was assumed to have a radius of 100 nm (Figure 5). The dielectric function for Au was taken from ref 49, and the permittivity of ta-C films was assumed to be 5.3. In the calculations the field enhancement refers to $(E/E_{in})^2$ with E_{in} being the incident field and is evaluated at $\lambda = 600$ nm, which is the dipole plasmon resonance wavelength of Au nanosphere. In Figure 5, the field enhancement factor $(E/E_{in})^2$ is plotted as a function of the distance from the sphere center ($Z = 0$) and center bias 10 nm ($Z = 10$ nm) and 20 nm ($Z = 20$ nm) of the Au sphere. It is seen that the field enhancement outside the surface of the Au sphere coated with ta-C film thickness of 1 nm is higher than that of the uncoated Au sphere. Furthermore, except for at the surface of substrates, Figure 5 also shows that the decrease of the field enhancement on the 1 nm ta-C coated Au sphere in the directions perpendicular to interface with distance from the surface is much slower than that of the uncoated Au nanosphere. The enhancement originates from the followings. First, this dielectric layer with a high refractive index can confine light field well. Because the dielectric layer is

ultrathin (up to 1 nm), it cannot confine this field wholly inside the dielectric. Instead, the interference of the scattered light from the inner and outer interfaces of the dielectric partly diminishes the optical field inside the layer. Because of the energy conservation, a relatively larger enhanced field is focused on the outer surface of the dielectric layer.[33]

Conclusions

It is worth noting that the enhancement of emission is obtained here from the fluorophores placed very close to the metal surface coated with the different thickness of ta-C layer, and this proposed strategy has several interesting following properties. First, the ta-C layer at about 10 Å can efficiently prevent the electron transfer from QDs excitation state to a metal so that the nonradiative decay can be reduced. At the same time, the metal substrate coated with 10 Å ta-C layer also shows a higher local electral field than the uncoated metal substrate. It will provide a maximum enhancement of radiative rate via the coupling between the emission of fluorophores and the local surface plasmon. Thus, we can get the maximum fluorescence enhancement by this stragety. In our experiment, a maximum enhancement factor of 64-fold is achieved at a thickness of 10 Å ta-C layer coated on the Au nanoparticles substrate, and even a single-molecule fluorescence enhancement should be realized if selecting a optimized radiating plasmonic metal structures, such as bowtie nanoantenna. Second, this strategy is available for any immobilized metal nanostructured substrates with different materials, shape, or size. Third, the coated substrate also has higher mechanical stability, chemical inertness, and technological compliance and may be useful, for example, to enhance TiO_2 photocatalysis and solar-cell efficiency by the surface plasmons. In summary, this strategy for enhancing the emission of fluorophores on the MEF substrate can be applied to a wide range of emitters and form a potential new platform for nanoscale photonics.

Acknowledgment. The authors gratefully acknowledge SAE Magnetics (H.K) Ltd. for DLC films coating and refractive index measurement. The work was sponsored by the State Key Program for Basic Research of China and NSFC under Grants 10734010, 50771054, and 10804044. This work was also supported in part by Jiang-Su planned projects for Postdoctoral Research Funds under Grant 0901015B.

Supporting Information Available: Postulated model of the effect of nonradiative decay process and the local electromagnetic field of ta-C coated substrates on the QDs PL intensity as a function of the ta-C spacer layer thickness; evaluation of the ta-C film coverage with different thicknesses by AES and XPS for the reference. This material is available free of charge via the Internet at http://pubs.acs.org.

References and Notes

(1) Barnes, W. L.; Dereux, A.; Ebbesen, T. W. *Nature* **2003**, *424*, 824.
(2) Nie, S. M.; Emory, S. R. *Science* **1997**, *275*, 1102.
(3) Kneipp, K.; Wang, Y.; Kneipp, H.; Perelman, L. T.; Dasari, R. R.; Feld, M. S. *Phys. Rev. Lett.* **1997**, *78*, 1667.
(4) Okamoto, K.; Niki, I.; Shvartser, A.; Narukawa, Y.; Mukai, T.; Scherer, A. *Nature Mater.* **2004**, *3*, 601.
(5) Lee, J.; Hernandez, P.; Lee, J.; Govorov, A. O.; Kotov, N. A. *Nature Mater.* **2007**, *6*, 291.
(6) Akimov, A. V.; Mukherjee, A.; Yu, C. L.; Chang, D. E.; Zibrov, A. S.; Hemmer, P. R.; Park, H.; Lukin, M. D. *Nature* **2007**, *450*, 402.
(7) Hakala, T. K.; Toppari, J. J.; Pettersson, M.; Kuzyk, A.; Tikkanen, H.; Kunttu, H.; Törmä, J. *Appl. Phys. Lett.* **2008**, *93*, 123307.
(8) Jin, Y. D.; Gao, X. H. *Nature Nanotechnol.* **2009**, *4*, 571.
(9) Wei, H.; Ratchford, D.; Li, X. Q.; Xu, H. X.; Shih, C. K. *Nano Lett.* **2009**, *9*, 4168.
(10) Aslan, K.; Leonenko, Z.; Lakowicz, J. R.; Geddes, C. D. *J. Fluoresc.* **2005**, *15*, 643.
(11) Carminati, R.; Greffet, J. J.; Henkel, C.; Vigoureux, J. M. *Opt. Commun.* **2006**, *261*, 368.
(12) Shimizu, K. T.; Woo, W. K.; Fisher, B. R.; Eisler, H. J.; Bawendi, M. G. *Phys. Rev. Lett.* **2002**, *89*, 117401.
(13) Ray, K.; Badugu, R.; Lakowicz, J. R. *J. Am. Chem. Soc.* **2006**, *128*, 8998.
(14) Kinkhabwala, A.; Yu, Z. F.; Fan, S. H.; Avlasevich, Y.; Müllen, K.; Moerner, W. E. *Nature Photonics* **2009**, *3*, 654.
(15) Muskens, O. L.; Giannini, V.; Snchez-Gil, J. A.; Gmez Rivas, J. *Nano Lett.* **2007**, *7*, 2871.
(16) Vecchi, G.; Giannini, V.; Gmez Rivas, J. *Phys. Rev. Lett.* **2009**, *102*, 146807.
(17) Mühlschlegel, P.; Eisler, H. J.; Martin, O. J. F.; Hecht, B.; Pohl, D. W. *Science* **2005**, *308*, 1607.
(18) Dulkeith, E.; Morteani, A. C.; Niedereichholz, T.; Klar, T. A.; Feldmann, J.; Levi, S. A.; van Veggel, F. C. J. M.; Reinhoudt, D. N.; Möller, M.; Gittins, D. I. *Phys. Rev. Lett.* **2002**, *89*, 203002.
(19) Soller, T.; Ringler, M.; Wunderlich, M.; Klar, T. A.; Feldmann, J.; Josel, H.-P.; Markert, Y.; Nichtl, A.; Kürzinger, K. *Nano Lett.* **2007**, *7*, 1941.
(20) Anger, P.; Bharadwaj, P.; Novotny, L. *Phys. Rev. Lett.* **2006**, *96*, 113002.
(21) Lin, H. Y.; Chen, Y. F.; Wu, J. G.; Wang, D. I.; Chen, C. C. *Appl. Phys. Lett.* **2006**, *88*, 161911.
(22) Pons, T.; Medintz, I. L.; Sapsford, K. E.; Higashiya, S.; Grimes, A. F.; English, D. S.; Mattoussi, H. *Nano Lett.* **2007**, *7*, 3157.
(23) Dubertret, B.; Calame, M.; Libchaber, A. J. *Nature Biotechnol.* **2001**, *19*, 365.
(24) Seelig, J.; Leslie, K.; Renn, A.; Kühn, S.; Jacobsen, V.; Corput, M.; Wyman, C.; Sandoghdar, V. *Nano Lett.* **2007**, *7*, 685.
(25) Lessard-Viger, M.; Rioux, M.; Rainville, L.; Boudreau, D. *Nano Lett.* **2009**, *9*, 3066.
(26) Sun, G.; Khurgin, J. B.; Soref, R. A. *Appl. Phys. Lett.* **2009**, *94*, 101103.
(27) Tovmachenko, O. G.; Graf, C.; van den Heuvel, D. J.; Blaaderen, A. V.; Gerritsen, H. C. *Adv. Mater.* **2006**, *18*, 91.
(28) Chen, Y. C.; Munechika, K.; Ginger, D. S. *Nano Lett.* **2007**, *7*, 690.
(29) Chen, C. W.; Wang, C. H.; Wei, C. M.; Chen, Y. F. *Appl. Phys. Lett.* **2009**, *94*, 071906.
(30) Bardhan, R.; Grady, N. K.; Halas, N. J. *Small* **2008**, *4*, 1716.
(31) Pompa, P. P.; Martiradonna, L.; Torre, A. D.; Sala, F. D.; Manna, L.; Vittorio, M. D.; Calabi, F.; Cingolani, R.; Rinaldi, R. *Nature Nanotechnol.* **2006**, *1*, 126.
(32) Feng, J. J.; Gernert, U.; Sezer, M.; Kuhlmann, U.; Murgida, D. H.; David, C.; Richter, M.; Knorr, A.; Hildebrandt, P.; Weidinger, I. M. *Nano Lett.* **2009**, *9*, 298.
(33) Xu, H. X. *Appl. Phys. Lett.* **2004**, *85*, 5980.
(34) Guo, S. H.; Tsai, S. J.; Kan, H. C.; Tsai, D. H.; Zacharich, M. R.; Phaneuf, R. J. *Adv. Mater.* **2008**, *20*, 1424.
(35) Jakob, M.; Levanon, H. *Nano Lett.* **2003**, *3*, 353.
(36) Standridge, S. D.; Schatz, G. C.; Hupp, J. T. *J. Am. Chem. Soc.* **2009**, *131*, 8407.
(37) Ferry, V. E.; Sweatlock, L. A.; Pacifici, D.; Atwater, H. A. *Nano Lett.* **2008**, *8*, 4391.
(38) Noginov, M. A.; Zhu, G.; Belgrave, A. M.; Shalaev, V. M.; Narimanov, E. E.; Stout, S.; Herz, E.; Suteewong, T.; Wiesner, U. *Nature* **2009**, *460*, 1110.
(39) Oulton, R. F.; Sorger, V. J.; Zentgraf, T.; Ma, R. M.; Gladden, C.; Dai, L.; Bartal, G.; Zhang, X. *Nature* **2009**, *461*, 629.
(40) Robertson, J. *Mater. Sci. Eng. R* **2002**, *37*, 129.
(41) Akita, N.; Konishi, Y.; Ogura, S.; Imamura, M.; Hu, Y. H.; Shi, X. *Diamond Relat. Mater.* **2001**, *10*, 1017.
(42) Liu, F. X.; Wang, Z. L. *Surf. Coat. Technol.* **2009**, *203*, 1829.
(43) Dearnaley, G.; Arps, H. J. *Surf. Coat. Technol.* **2005**, *200*, 2518.
(44) Fedel, M.; Motta, A.; Maniglio, D.; Migliaresi, C. *J. Biomed. Mater. Res., Part B: Appl. Biomater.* **2008**, 338.
(45) Zhan, P.; Wang, Z. L.; Dong, H.; Sun, J.; Wu, J.; Wang, H. T.; Zhu, S. N.; Zi, J. *Adv. Mater.* **2006**, *18*, 1612.
(46) Christy, L. H.; Van Duyne, R. P. *J. Phys. Chem. B* **2001**, *105*, 5599.
(47) Murray, W. A.; Suckling, J. R.; Barnes, W. L. *Nano Lett.* **2006**, *6*, 1772.
(48) Farcǔ, C.; Astilean, S. *Appl. Phys. Lett.* **2009**, *95*, 193110.
(49) Johnson, P. B.; Christy, R. W. *Phys. Rev. B* **1972**, *6*, 4370.

JP101767Z